

Eigenmodes and resonance vibrations of 2D nanomembranes – Graphene and hexagonal boron-nitride

Alexander V. Savin¹

¹ *N.N. Semenov Federal Research Center for Chemical Physics,
Russian Academy of Sciences (FRCCP RAS), Moscow, 119991, Russia*

Natural and resonant oscillations of suspended circular graphene and hexagonal boron nitride (h-BN) membranes (single-layer sheets lying on a flat substrate having a circular hole of radius R) have been simulated using full-atomic models. Substrates formed by flat surfaces of graphite and h-BN crystal, hexagonal ice, silicon carbide 6H-SiC and nickel surface (111) have been used. The presence of the substrate leads to the forming of a gap at the bottom of the frequency spectrum of transversal vibrations of the sheet. The frequencies of natural oscillations of the membrane (oscillations localized on the suspended section of the sheet) always lie in this gap, and the frequencies of oscillations decrease by increasing radius of the membrane as $(R + R_i)^{-2}$ with nonzero effective increase of radius $R_i > 0$. The modeling of the sheet dynamics has shown that small periodic transversal displacements of the substrate lead to resonant vibrations of the membranes at frequencies close to eigenfrequencies of nodeless vibrations of membranes with a circular symmetry. The energy distribution of resonant vibrations of the membrane has a circular symmetry and several nodal circles, whose number i coincides with the number of the resonant frequency. The frequencies of the resonances decrease by increasing the radius of the membrane as $(R + R_i)^{\alpha_i}$ with exponent $\alpha_i < 2$. The lower rate of resonance frequency decrease is caused by the anharmonicity of membrane vibrations.

I. INTRODUCTION

Being a nanosized polymorph of carbon, graphene attracts increased attention of researchers due to its unique physical properties [1, 2]. The remarkable properties of graphene have enabled the exploitation of graphene for the development of nano-electro-mechanical system (NEMS) such as nanoresonators [3, 4]. The vibrational properties of graphene play an important role in analysis and design of graphene-based sensors and resonators. The aim of this work is to simulate the eigenmodes and resonant vibrations of suspended circular graphene (G) and hexagonal boron nitride (h-BN) membranes. Such 2D membranes are formed as single-layer G and h-BN sheets lying on a flat substrate with a circular hole – see Fig. 1. These one atom thick membranes can be used as highly efficient nanomechanical resonators [5–9] and as extraordinary sensitive detectors of mass, force and pressure [10–12].

For analysis of vibrations of such membranes continuum models in which a sheet of graphene is considered as continuous thin plate or thin shell [13–16] are usually used. In this paper we will use discrete (full-atomic) models that take into account the hexagonal structure of the sheets. As substrate, we consider the plane surfaces of an ideal graphite and h-BN crystals, hexagonal ice I_h , silicon carbide 6H-SiC and the surface (111) of Nickel crystal.

II. MODEL

To calculate the interaction energy of a sheet (graphene and h-BN) with a flat substrate the sheet has been placed parallel to the substrate surface. The interaction poten-

tial of each atom belonging to the sheet with the substrate $W(h)$ can be found as the function of the distance to the substrate plane h , as a sum of its interaction energies with the substrate atoms. The interaction of pairs of atoms has been described by the Lennard-Jones (LJ) potential (6,12):

$$V_{LJ}(r) = \epsilon_0[(r_0/r)^{12} - 2(r_0/r)^6], \quad (1)$$

where ϵ_0 is the binding energy and r_0 is the bond length. To find the interaction energy of graphene with the crystalline graphite surface, we used the potential parameters taken from [17] and, for other substrates, from [18]. Table I shows the parameters of LJ potential (1) for various atomic pairs.

The calculations have been made for the $2.0 \times 1.8 \text{ nm}^2$ graphene (h-BN) sheet consisting of 160 carbon (boron and nitride) atoms, which is arranged in parallel to the crystal surface at distance h . At each value of distance h , the energy was averaged over the shifts along substrate surface and, then, normalized on the number of atoms in the graphene (h-BN) sheet. As a result, we obtained the dependence of the interaction energy of one atom of the sheet with the substrate on its distance from substrate plane $W(h)$. The calculations showed that the interaction energy with the substrate $W(h)$ can be described with a high accuracy by the Lennard-Jones potential (k, l):

$$W(h) = \epsilon_1[k(h_1/h)^l - l(h_1/h)^k]/(l - k), \quad (2)$$

where power $l > k$. Potential (2) has the minimum $W(h_1) = -\epsilon_1$ (ϵ_1 is the binding energy of the atom with substrate). The stiffness of interaction with the substrate is $K_1 = W''(h_1) = \epsilon_1 lk/h_1^2$. Table II presents the parameters of LJ potential (2) for graphene and h-BN sheet on various substrates.

Table I: Parameters of the LJ potential (1) for various pairs of interacting atoms.

	[17] CC	[18] CC	CH	CO	CSi	NO	NH	NC	NSi	BO	BH	BC	BSi
ϵ_0 (meV)	2.76	4.56	2.95	3.44	8.92	2.78	2.38	3.69	7.24	4.51	3.86	5.94	11.66
r_0 (Å)	3.809	3.851	3.369	3.676	4.073	3.579	3.25	3.754	3.965	3.78	3.433	3.965	4.188

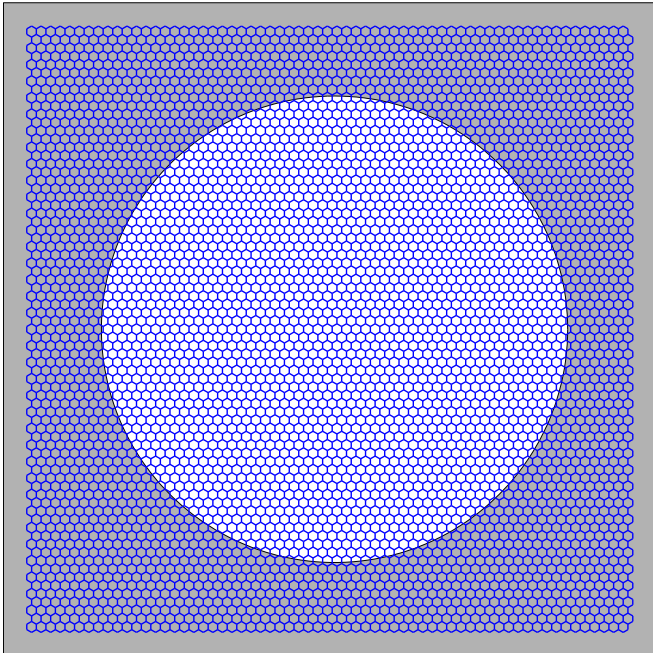


Figure 1: The rectangular sheet of graphene lying on a flat substrate having a circular hole in its center. The sheet consists of 9470 carbon atoms and has the shape of a rectangle of size $15.6 \times 15.6 \text{ nm}^2$. The radius of the hole in the substrate $R = 6 \text{ nm}$.

Table II: Parameters of (k, l) LJ potential (2) for graphene and h-BN sheets on various substrates.

	ϵ_1 (eV)	h_1 (Å)	l	k	K_1 (N/m)
Graphene – Ice I_h	0.029	3.005	10	3.5	1.80
Graphene – Graphite	0.052	3.37	10	3.75	2.75
Graphene – 6H-SiC	0.073	4.19	17	3.75	4.24
Graphene – h-BN	0.0903	3.46	10	3.75	4.53
h-BN – Ice I_h	0.0304	3.04	10	3.5	1.81
h-BN – 6H-SiC	0.0803	4.20	17	3.75	4.50

When graphene is located on the surface (111) of crystalline nickel, a stronger chemical interaction of carbon atoms with the atoms of the substrate occurs (hybridization of the metal d -band with graphene π -states and charge transfer from the metal to graphene). As a result of the interaction of a graphene sheet with a crystal surface a gap of the magnitude $\omega_0 = 240 \text{ cm}^{-1}$ appears at the bottom of the frequency spectrum of transversal oscillations of the sheet [19]. From this we can estimate

the harmonic coupling parameter of the interaction of the sheet atom with the substrate $K_1 = \omega_0^2 M_C = 41 \text{ N/m}$ (M_C is the mass of carbon atom). Therefore, for small displacements, the interaction with the substrate can be described by the harmonic potential

$$W(h) = \frac{1}{2} K_1 (h - h_1)^2, \quad (3)$$

with stiffness coefficient $K_1 = 41 \text{ N/m}$ and equilibrium distance to the substrate plane $h_1 = 2.145 \text{ Å}$ [20].

To describe oscillations of the graphene and h-BN sheet, we present the system Hamiltonian in the form,

$$H = \sum_{n=1}^N \left[\frac{1}{2} M_n (\dot{\mathbf{u}}_n, \dot{\mathbf{u}}_n) + P_n + \delta_n W(z_n) \right], \quad (4)$$

where M_n is the mass of n -th atom of the sheet, $\mathbf{u}_n = (x_n(t), y_n(t), z_n(t))$ is the radius-vector of n -th atom at the time t . The term P_n describes the energy of interaction of the atom with index n with the neighboring atoms, term $W(z_n)$ – the energy of interaction of the atom with substrate surface (the plane of the substrate coincides with the plane xy). Coefficient $\delta_n = 1$ if n -th atom interacts and $\delta_n = 0$ if it does not interact with the substrate (if it lies above the hole in the substrate).

To describe the dynamics of a graphene sheet, we used the interaction potentials described in detail in [21, 22], whereas to describe monolayer hexagonal boron nitride (h-BN) sheet we used extended Tersoff potential [23].

We consider a hydrogen-terminated graphene (h-BN) sheet, where edge atoms correspond to the molecular group CH (BH or NH). We consider such a group as a single effective particle at the location of the carbon atom. Therefore, in our model of graphene nanoribbons we take the mass of atoms inside the stripe as $M_n = 12m_p$, and for the edge atoms we consider a larger mass $M_n = 13m_p$ (where $m_p = 1.6603 \cdot 10^{-27} \text{ kg}$ is the proton mass).

If we want to simulate the absence of a substrate for a part of the sheet atoms, we must take $\delta_n = 0$ for these atoms. Figure 1 shows a square sheet of graphene of size $15.6 \times 15.6 \text{ nm}^2$ consisting of $N = 9470$ carbon atoms. The central circular part of the sheet does not interact with the substrate (for atoms from this part the coefficient $\delta_n = 0$), forming a circular membrane of radius $R = 6 \text{ nm}$. A similar structure was used to model the vibrations of a circular membrane made of h-BN sheet.

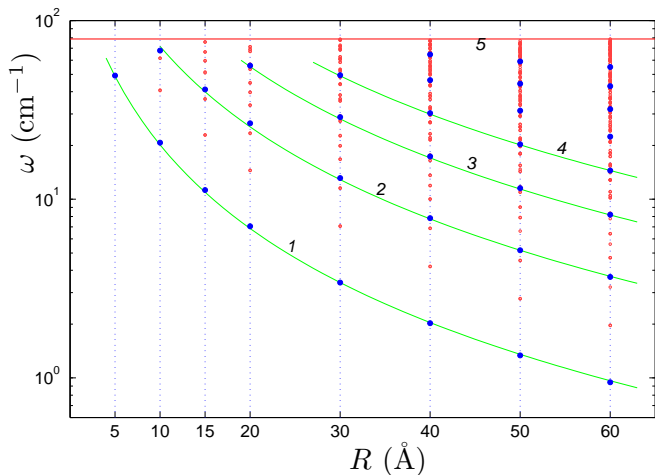


Figure 2: Dependence of frequencies ω of intrinsic transversal oscillations of a circular membrane of a graphene sheet lying on the surface of crystalline h-BN substrate on the radius of the membrane R . Curves $i = 1, 2, 3, 4$ show the dependencies $\omega_i = c_i/(R + R_i)^2$, where coefficients $c_i = 3950, 15500, 34500, 62500 \text{ cm}^{-1}\text{\AA}^2$, additional radius $R_i = 4.0, 4.7, 5.0, 5.7 \text{ \AA}$. Straight line 5 shows the minimum frequency of transversal oscillations of a graphene sheet on a flat substrate $\omega = \omega_0 = 78.87 \text{ cm}^{-1}$. Large markers show natural frequencies of intrinsic nodeless oscillations of the membrane with circular symmetry.

III. TRANSVERSAL NORMAL MODES

Let us consider the transversal vibrations of the atoms of the sheet. The natural frequencies and normal modes were derived numerically as the solution of the problem on eigenvalues for matrices of the second derivatives of size $N \times N$.

When only transversal offsets are taken into account, the Hamiltonian of the sheet (4) can be written in the form

$$H = \frac{1}{2}(\mathbf{M}\dot{\mathbf{Z}}, \dot{\mathbf{Z}}) + \mathcal{P}(\mathbf{Z}), \quad (5)$$

where \mathbf{M} is a diagonal matrix of all masses of the sheet, $\mathbf{Z} = \{z_n - h_0\}_{n=1}^N$ is N -dimensional vector of transversal displacements from equilibrium positions. Hamiltonian (5) corresponds to the motion equations,

$$-\mathbf{M}\ddot{\mathbf{Z}} = \frac{\partial}{\partial \mathbf{Z}}\mathcal{P}(\mathbf{Z}). \quad (6)$$

For small displacements, Eq. (6) reduces to a system of linear equations,

$$-\mathbf{M}\ddot{\mathbf{Z}} = \mathbf{B}\mathbf{Z}, \quad (7)$$

where the matrix has dimension $N \times N$,

$$\mathbf{B} = \left(\frac{\partial^2 \mathcal{P}}{\partial z_{n_1} \partial z_{n_2}} \Big|_{\mathbf{Z}=0} \right)_{n_1=1, n_2=1}^{N, N}.$$

Next, we make the transformation $\mathbf{Z} = \mathbf{M}^{-1/2}\mathbf{X}$, and reduce the system (7) to the linear equations of the form $-\ddot{\mathbf{X}} = \mathbf{C}\mathbf{X}$ with the symmetric matrix $\mathbf{C} = \mathbf{M}^{-1/2}\mathbf{B}\mathbf{M}^{-1/2}$. Solutions of this linear system describe the eigenmodes of the sheet oscillations, which can be presented in the form $\mathbf{X}(t) = \mathbf{A}\mathbf{e}\exp(i\omega t)$, where A is the oscillation amplitude, $\omega = \sqrt{\lambda}$ is the frequency, λ and \mathbf{e} are the eigenvalue and normalized eigenvector of the matrix \mathbf{C} [$\mathbf{C}\mathbf{e} = \lambda\mathbf{e}$, $(\mathbf{e}, \mathbf{e}) = 1$].

The eigenvalues of the matrix \mathbf{C} can be found numerically. Numerical matrix diagonalization demonstrates that the presence of the substrate leads to the presence of the gap $[0, \omega_0]$ at the bottom of the frequency spectrum of transversal vibrations (minimum nonzero frequency $\omega_0 = \sqrt{K_1/M}$, for graphene $M = M_C$). All eigen transversal vibrations of the sheet with frequencies $\omega < \omega_0$ correspond to vibrations localized in the suspended central part of the sheet, i.e. to eigen vibrations of the circular membrane.

The dependence of the natural oscillations of the circular membrane on its radius is shown in Fig. 2. Here, frequency $\omega_0 = 78.87 \text{ cm}^{-1}$. A graphene membrane on a crystalline h-BN substrate with a radius of the central hole in the substrate $R = 5$ has only one localized natural oscillation, at $R = 10 - 6$ oscillations, at $R = 15 - 14$, at $R = 20 - 23$, at $R = 30 - 55$, at $R = 40 - 94$, at $R = 50 - 144$ and at $R = 60 \text{ \AA} - 209$ natural oscillations. The minimum natural frequency of transversal vibrations of the membrane is approximated with high accuracy by the dependence

$$\omega_i \sim c_i/(R + R_i)^2, \quad (8)$$

with index $i = 1$, $c_1 = 3950 \text{ cm}^{-1}\cdot\text{\AA}^2$, $R_1 = 4.0 \text{ \AA}$.

Asymptotics (8) take place for all substrates, it shows that the interaction of the sheet with the substrate leads to an additional "increase" of the effective radius of the membrane on R_i . The amount of additional magnification depends on the force of interaction with the substrate. The stronger is the interaction with the substrate, the smaller is the value of R_1 . So $R_1 = 4.7$ for ice substrate having the weakest interaction with a sheet, $R_1 = 4.2$ for graphite substrate, $R_1 = 3.8$ for silicon carbide substrate, and $R_1 = 2.1 \text{ \AA}$ for substrate with the strongest interaction Ni (111).

Higher frequency natural nodeless oscillations of the membrane with circular symmetry also have asymptotic (8) with index $i = 2, 3, \dots$ - see Fig. 2.

IV. ANHARMONISM OF MEMBRANE VIBRATIONS

To simulate the natural vibrations of the membrane, we must numerically integrate a system of equations of motion

$$M_n \ddot{\mathbf{u}}_n = -\frac{\partial H}{\partial \mathbf{u}_n}, \quad n = 1, \dots, N, \quad (9)$$

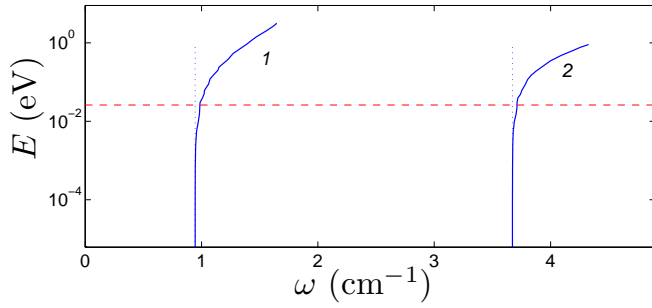


Figure 3: Dependence of frequencies ω of the first and the second (curves 1 and 2) natural oscillations of the circular membrane ($R = 6$ nm) on energy of vibration E . Energy of thermal vibrations $E = k_B T$ for temperature $T = 300$ K is represented by a horizontal dashed line.

with initial conditions

$$\begin{aligned} x_n(0) &= x_n^0, & y_n(0) &= y_n^0, & z_n(0) &= z_n^0, \\ \dot{x}_n(0) &= 0, & \dot{y}_n(0) &= 0, & \dot{z}_n(0) &= A e_n, \end{aligned}$$

where $\{\mathbf{u}_n^0 = (x_n^0, y_n^0, z_n^0)\}_{n=1}^N$ is the ground state of the graphene sheet, $\mathbf{e} = \{e_n\}_{n=1}^N$ is the eigenvector of the matrix \mathbf{C} (amplitude A determines the energy of vibrations $E = A^2(\mathbf{M}\mathbf{e}, \mathbf{e})/2$). We will use the condition of absorbing edges (the friction $\Gamma = 1/t_r$ with time relaxation $t_r = 10$ ps was introduced on edges of the sheet).

Let us consider the dynamics of the natural vibration of the membrane with radius $R = 60$ Å. Numerical integration of the system of equations of motion (9) has shown that when energy $E < E_0 = 0.01$ eV the membrane performs harmonic oscillations with eigen mode frequency (frequency of the vibration ω does not depend on the energy E). When $E > E_0$, the frequency of the membrane vibration begins to increase monotonically when increasing energy – see Fig. 3. Thus, at high energy, the membrane behaves as anharmonic oscillator with rigid anharmonicity. Let us note that at room temperature $T = 300$ K, the energy of thermal self-oscillation of the membrane $E > E_0$ ($E = k_B T = 0.026$ eV). Therefore, at room temperature, the thermal vibrations of the graphene membrane will be anharmonic.

V. RESONANT VIBRATIONS

To analyze the resonant vibrations of a single-layer membrane, we will simulate the effect of periodic transversal changes in the position of the substrate on its vibrations. To do this, we numerically integrate the system of Langevin equations of motion

$$\begin{aligned} M_n \ddot{x}_n &= -\frac{\partial H}{\partial x_n} + \delta_n [-\Gamma M_n \dot{x}_n + \xi_{n,1}(t)], \\ M_n \ddot{y}_n &= -\frac{\partial H}{\partial y_n} + \delta_n [-\Gamma M_n \dot{y}_n + \xi_{n,2}(t)], \end{aligned} \quad (10)$$

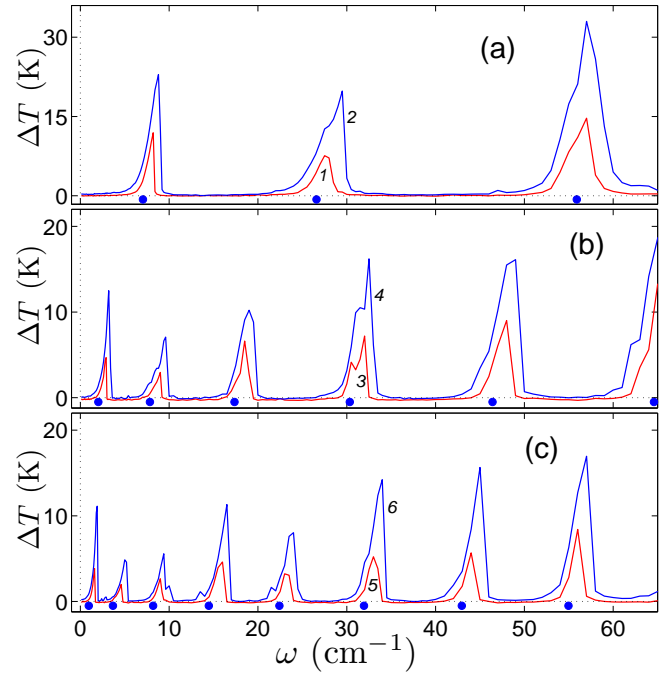


Figure 4: Dependence of additional thermalization of the graphene membrane ΔT on the oscillation frequency of the h-BN substrate ω for (a) membrane radius $R = 2$, (b) $R = 4$ and (c) $R = 6$ nm. Red curves 1, 3, 5 show dependencies for amplitude of forced substrate vibrations $A = 1$, blue curves 2, 4, 6 – dependencies for $A = 2$ Å·cm⁻¹. The circular markers show the values of the frequencies of the intrinsic nodeless oscillations of the membrane with circular symmetry.

$$M_n \ddot{z}_n = -\frac{\partial H}{\partial z_n} + \delta_n [-\Gamma M_n \dot{z}_n + \xi_{n,3}(t) + F(t, z_n)],$$

where the coefficient $\delta_n = 1$ if the atom interacts with the substrate and $\delta_n = 0$ if it does not interact (if it is located in the suspended part of the sheet), $\Gamma = 1/t_r$ is the friction coefficient, and random forces vectors $(\xi_{n,1}, \xi_{n,2}, \xi_{n,3})$ are normalized as follows:

$$\langle \xi_{n,i}(t_1) \xi_{m,j}(t_2) \rangle = 2M_n \Gamma k_B T \delta_{nm} \delta_{ij} \delta(t_1 - t_2),$$

k_B – Boltzmann constant, T – temperature of the thermostat, F – force of attraction of the atom to the substrate.

If the position of the substrate plane is periodically changed along the z axis, then in the system of sheet motion equations (10) the force

$$F(t, z) = -W'(z + \frac{A}{\omega} \cos(\omega t)),$$

where A and ω – the amplitude and the frequency of the forced oscillations of the substrate (by this definition the amplitude A characterizes the oscillation energy).

Let us analyze at what frequencies of forced oscillations of the substrate pumping of the energy to vibrations of the suspended section of the sheet will be the highest.

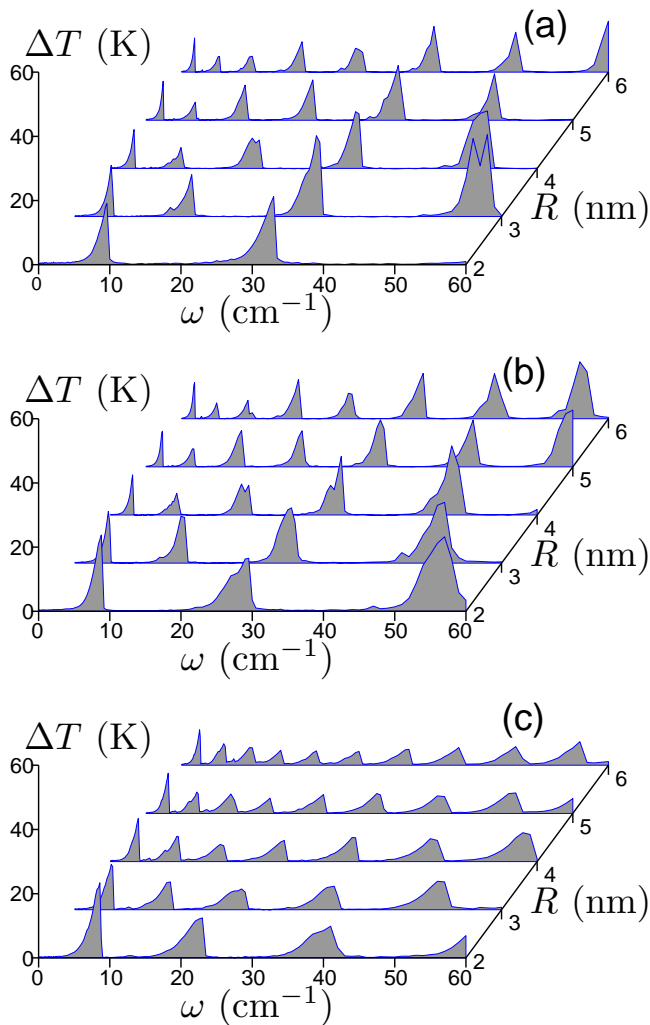


Figure 5: Dependence of additional thermalization ΔT on the oscillation frequency of the substrate ω and on the membrane radius R for graphene membrane on substrates (a) Ni(111), (b) 6H-SiC(0001) and (c) for h-BN membrane on the substrate 6H-SiC(0001) (amplitude $A = 2 \text{ \AA} \cdot \text{cm}^{-1}$).

For the sheet, the substrate is an external thermostat, so in the system of the equations of motion (10) only atoms in contact with the substrate interact with the Langevin thermostat. The intensity of heat exchange with the thermostat is characterized by a relaxation time t_r . The value $t_r = 1 \text{ ps}$ was used in the simulation. In the time $t_0 = 100t_r$ the sheet being fully thermalized. The analysis of the further dynamics of the sheet allows us to find the average temperature of the circular membrane

$$T_m = \frac{1}{3N_m k_B} \sum_{n=1}^N (1-\delta_n) M_n \langle (\dot{\mathbf{u}}_n, \dot{\mathbf{u}}_n) \rangle, \quad N_m = \sum_{n=1}^N (1-\delta_n),$$

where summation occurs only for atoms not in contact with the substrate (N_m is the number of such atoms),

and the average value

$$\langle (\dot{\mathbf{u}}_n, \dot{\mathbf{u}}_n) \rangle = \lim_{t \rightarrow \infty} \frac{1}{t} \int_{t_0}^{t_0+t} (\dot{\mathbf{u}}_n(\tau), \dot{\mathbf{u}}_n(\tau)) d\tau.$$

When the substrate is stationary (when the oscillation amplitude $A = 0$), the temperature of the membrane is always equal to the temperature of the thermostat ($T_m = T$). Therefore, additional thermalization of the membrane can be characterized by a temperature difference $\Delta T = T_m - T$.

Let us take the oscillation amplitude $A = 1, 2 \text{ \AA} \cdot \text{cm}^{-1}$, the temperature of the thermostat $T = 300 \text{ K}$. The dependence of the additional thermalization of the membrane ΔT on the frequency of vertical oscillations of the substrate ω is shown in Fig. 4. As can be seen from the figure, the additional thermalization of the membrane is different from zero only near certain frequency values, the number of which increases with increasing membrane radius (see Fig. 5). Because by the vertical displacement of the substrate on all the edge atoms of the circular membrane are the same forces, the vertical vibrations of the substrate in the membrane can only cause vibrations with circular symmetry. Therefore, additional thermalization occurs only at frequencies close to the frequencies of the intrinsic nodeless oscillations of the membrane, which have a circular symmetry (the amplitude of the displacements of the membrane atom depends only on its distance from the center of the membrane). Thus, additional thermalization of the membrane occurs primarily due to the resonant pumping of its own circularly symmetric oscillations.

A similar resonant pumping of the membrane eigenmodes occurs for the graphene and h-BN sheets for all considered substrates – see Fig. 5. As can be seen from the figure, the resonant pumping of the main oscillation occurs almost equally for all membranes. The differences appear only for higher frequency resonances. As the membrane radius increases, the resonance frequencies decrease and their number increases. The analysis of the energy distribution of resonant vibrations of the membrane (see Fig. 6) shows that the distribution always has a circular symmetry and has several nodal circles whose number coincides with the number of the resonance frequency. This shows that resonance pumping occurs primarily due to the excitation of natural oscillations of the membrane with circular symmetry (i.e. oscillations having only nodal circles).

Let us consider in more detail the first resonance of the membrane. As can be seen in Fig. 4 and 5, when the frequency increases, the vibrational energy of the membrane initially grows monotonically, at a certain frequency ω_r reaches its maximum value, and then sharply decreases to the background value of the energy of thermal vibrations. Therefore, it is convenient to determine the frequency of the first resonance as the average value

$$\bar{\omega}_1 = \frac{1}{C} \int_0^{1.1\omega_r} \omega \Delta T(\omega) d\omega, \quad C = \int_0^{1.1\omega_r} \Delta T(\omega) d\omega.$$

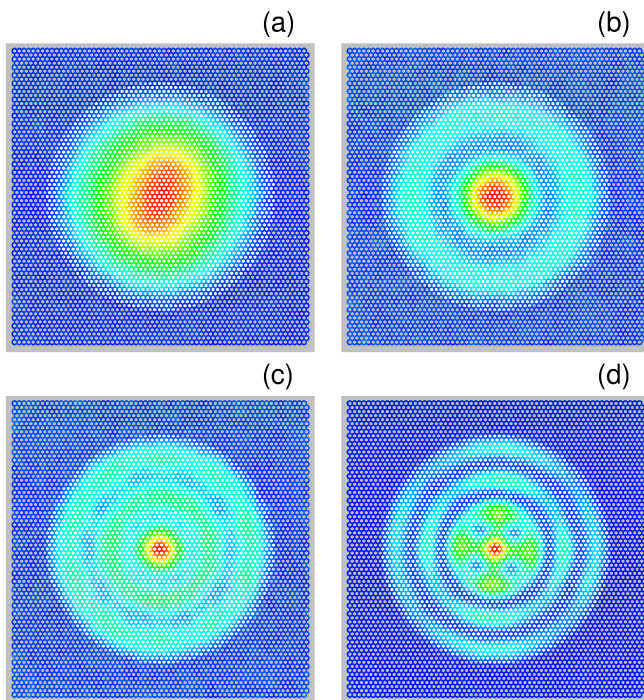


Figure 6: Temperature distribution in a circular graphene membrane of radius $R = 6$ nm (h-BN substrate, amplitude of forced substrate oscillations $A = 2 \text{ \AA} \cdot \text{cm}^{-1}$) at: (a) first resonance (frequency $\omega = 1.9 \text{ cm}^{-1}$, maximum temperature $T_m = 331\text{K}$); (b) second resonance ($\omega = 5.0 \text{ cm}^{-1}$, $T_m = 324\text{K}$); (c) third resonance ($\omega = 9.4 \text{ cm}^{-1}$, $T_m = 324\text{K}$); (d) the fourth resonance ($\omega = 16.5 \text{ cm}^{-1}$, $T_m = 366\text{K}$). Blue color corresponds to the background temperature $T = 300\text{K}$, red color corresponds to the maximum temperature T_m .

Similarly, we can define the frequencies of next resonances $\bar{\omega}_i$, $i = 2, 3, \dots$

The results of numerical simulation of membrane vibrations are shown in Fig. 4. The figure shows that each i -th eigen membrane vibration with a circular (radial) symmetry corresponds to resonant membrane vibration with frequency $\bar{\omega}_i > \omega_i$. The resonance frequency is always higher than the frequency of the corresponding natural membrane vibration but lower than the frequency of the next natural vibration: $\omega_i < \bar{\omega}_i < \omega_{i+1}$, $i = 1, 2, 3, \dots$. The larger the amplitude A of forced substrate vibration gets, the stronger the resonance frequency shifts to the right. This indicates the nonlinearity of resonances due to rigid anharmonicity of membrane natural vibration at high energy (the frequency of natural vibration increases with increasing vibration amplitude).

The analysis of dependency of the resonance frequency $\bar{\omega}_i$ on membrane radius R shows that as the radius increases, the resonance frequency decreases slower than the frequency of the corresponding natural membrane vibration ω_i :

$$\bar{\omega}_i \sim d_i / (R + R_i)^{\alpha_i}, \quad \alpha_i < 2, \quad (11)$$

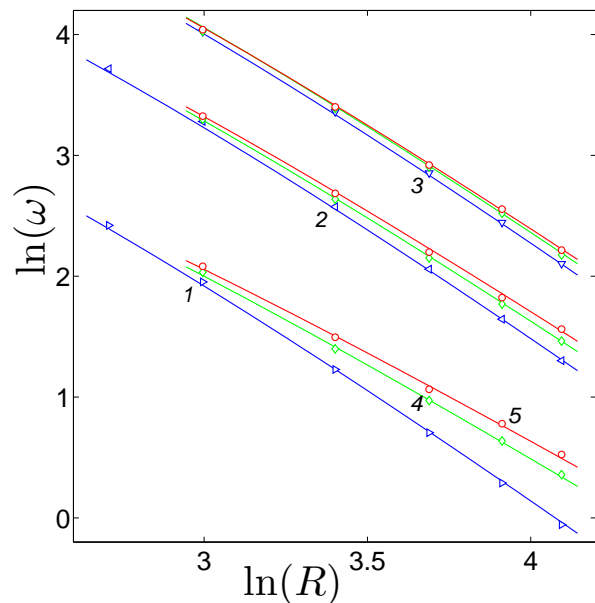


Figure 7: Dependence of oscillation frequencies ω_i ($i = 1, 2, 3$, markers 1, 2, 3) and resonance frequencies $\bar{\omega}_i$ on membrane radius R for graphene on h-BN substrate. Blue curves 1, 2, 3 give approximations $\omega_i = c_i / (R + R_i)^2$, $c_i = 3950, 15500, 34500 \text{ cm}^{-1} \cdot \text{\AA}^2$, $R_i = 4.0, 4.7, 5.0 \text{ \AA}$, $i = 1, 2, 3$. Markers 4 give resonance frequencies $\bar{\omega}_i$ for amplitude of forced substrate vibrations $A = 1$, markers 5 – for $A = 2 \text{ \AA} \cdot \text{cm}^{-1}$. Green curves give approximations $\bar{\omega}_i = d_i / (R + R_i)^{\alpha_i}$ for $A = 1$ ($d_i = 1650, 11900, 32000$, $\alpha_i = 1.7, 1.9, 1.96$), red curves – for $A = 2$ ($d_i = 1270, 10500, 2800 \text{ cm}^{-1} \cdot \text{\AA}^{\alpha_i}$, $\alpha_i = 1.6, 1.85, 1.92$). Dimension of the frequency $[\omega] = \text{cm}^{-1}$, radius $[R] = \text{\AA}$.

– see Fig. 7. The greater the amplitude A of the substrate oscillation, the lower the value of exponent α_i . For the first resonance ($i = 1$) the exponent $\alpha_1 = 1.7$ for $A = 1$, and $\alpha_i = 1.6$ for $A = 2 \text{ \AA} \cdot \text{cm}^{-1}$. The deceleration of the decrease of the resonance frequencies $\bar{\omega}_i$ with increasing radius R is caused by the anharmonicity of the membrane vibrations.

VI. CONCLUSIONS

We have simulated natural and resonant oscillations of suspended circular graphene and hexagonal boron nitride (h-BN) membranes using full-atomic models. The presence of the substrate (of flat surface of graphite and h-BN crystal, hexagonal ice, silicon carbide 6H-SiC(0001), nickel surface (111)) leads to the forming of a gap at the bottom of the frequency spectrum of transversal vibrations of the sheet. Frequencies of natural oscillations of the membrane ω_i always lie in this gap, and they decrease with the increasing radius of the membrane R as $(R + R_i)^{-2}$ with nonzero effective increase of radius $R_i > 0$. The modeling of the sheet dynamics has shown that small periodic transversal displacements of

the substrate lead to resonant vibrations of the membranes, at frequencies close to the eigenfrequencies of nodeless vibrations of the membranes with circular symmetry. The energy distribution of the resonant vibrations of the membrane has a circular symmetry and several nodal circles whose number coincides with the number of the resonant frequency i . The frequencies of the resonances decrease by increasing the radius of the membrane as $(R + R_i)^{\alpha_i}$ with exponent $\alpha_i < 2$. The lower rate of the resonance frequency decrease is caused by the anharmonicity of membrane vibrations.

Acknowledgements

The author thanks Yuri S. Kivshar for formulating this problem. This work was supported by the Russian Foundation for Basic Research, Grant No. 18-29-19135. Computational facilities were provided by the Interdepartmental Supercomputer Center of the Russian Academy of Sciences.

-
- [1] A. K. Geim and K. S. Novoselov. The rise of graphene. *Nat. Mater.* **6**, 183 (2007).
- [2] C. Soldano, A. Mahmood, and E. Dujardin. Production, properties and potential of graphene. *Carbon* **48**, 2127 (2010).
- [3] J. S. Bunch, A. M. van der Zande, S. S. Verbridge, I. W. Frank, D. M. Tanenbaum, J. M. Parpia, H. G. Craighead, and P. L. McEuen. Electromechanical Resonators from Graphene Sheets. *Science* **315**, 490 (2007).
- [4] K. Eom, H. S. Park, D. S. Yoon, and T. Kwon. Nanomechanical resonators and their applications in biological/chemical detection: nanomechanics principles. *Phys. Rep.* **503**, 115-163 (2011).
- [5] A. M. van der Zande, R. A. Barton, J. S. Alden, C. S. Ruiz-Vargas, W. S. Whitney, P. H. Q. Pham, J. Park, J. M. Parpia, H. G. Craighead, and P. L. McEuen. Large-Scale Arrays of Single-Layer Graphene Resonators. *Nano Lett.* **10**, 4869-4873 (2010).
- [6] R. A. Barton, B. Ilic, A. M. van der Zande, W. S. Whitney, P. L. McEuen, J. M. Parpia, and H. G. Craighead. High, Size-Dependent Quality Factor in an Array of Graphene Mechanical Resonators. *Nano Lett.* **11**, 1232-1236 (2011).
- [7] R. A. Barton, J. Parpia, H. G. Craighead. Fabrication and performance of graphene nanoelectromechanical systems. *J. Vac. Sci. Technol. B* **29**(5), 050801 (2011).
- [8] J. Güttinger, A. Noury, P. Weber, A. M. Eriksson, C. Lagoin, J. Moser, C. Eichler, A. Wallraff, A. Isacsson and A. Bachtold. Energy-dependent path of dissipation in nanomechanical resonators. *Nature Nanotechnology* **12**, 631-636 (2017).
- [9] G. J. Verbiest, J. N. Kirchhof, J. Sonntag, M. Goldsche, T. Khodkov and C. Stampfer. Detecting Ultrasound Vibrations with Graphene Resonators. *Nano Lett.* **18**, 5132-5137 (2018).
- [10] J. S. Bunch, S. S. Verbridge, J. S. Alden, A. M. van der Zande, J. M. Parpia, H. G. Craighead, and P. L. McEuen. Impermeable Atomic Membranes from Graphene Sheets. *Nano Lett.* **8**(8), 2458-2462 (2008).
- [11] A. D. Smith, F. Niklaus, A. Paussa, S. Schröder, A. C. Fischer, M. Sterner, S. Wagner, S. Vaziri, F. Forsberg, D. Esseni, M. Östling, and M. C. Lemme. Piezoresistive Properties of Suspended Graphene Membranes under Uniaxial and Biaxial Strain in Nanoelectromechanical Pressure Sensors. *ACS Nano* **10**(11), 9879-9886 (2016).
- [12] D. Akinwande, C. J. Brennan, J. S. Bunch, P. Egberts, J. R. Felts, H. Gao, R. Huang, J.-S. Kim, T. Li, Y. Li, K. M. Liechti, N. Lu, H. S. Park, E. J. Reed, P. Wang, B. I. Yakobson, T. Zhang, Y.-W. Zhang, Y. Zhou, Y. Zhu. A review on mechanics and mechanical properties of 2D materials—Graphene and beyond. *Extreme Mechanics Letters* **13**, 42-77 (2017)
- [13] J. Atalaya, A. Isacsson, and J. M. Kinaret. Continuum Elastic Modeling of Graphene Resonators. *Nano Lett.* **8**(12), 4196-4200 (2008).
- [14] M. D. Dai, C.-W. Kim, and K. Eom. Nonlinear vibration behavior of graphene resonators and their applications in sensitive mass detection. *Nanoscale Research Letters* **7**, 499 (2012).
- [15] R. Ghaffari, R. A. Sauer. Modal analysis of graphene-based structures for large deformations, contact and material nonlinearities. *Journal of Sound and Vibration* **423** 161-179 (2018).
- [16] F.-T. Shi, S.-C. Fan, C. Li, and Z.-A. Li. Opto-thermally excited Fabry-Perot resonance frequency behaviors of clamped circular graphene membrane. *Nanomaterials* **9**, 563 (2019).
- [17] R. Setton. Carbon nanotubes – II. Cohesion and formation energy of cylindrical nanotubes. *Carbon* **34**, 69–75 (1996).
- [18] A.K. Rappe, C.J. Casewit, K.S. Colwell, W.A. Goddard III, and W.M. Skiff. UFF, a full periodic table force field for molecular mechanics and molecular dynamics simulations. *J. Am. Chem. Soc.* **114**, 10024-10035 (1992).
- [19] A. Dahal and M. Batzill. Graphene-nickel interfaces: a review. *Nanoscale* **6**, 2548 (2014).
- [20] Y. Gamo, A. Nagashima, M. Wakabayashi, M. Terai and C. Oshima. Atomic structure of monolayer graphite formed on Ni(111). *Surf. Sci.* **374**, 61-64 (1997).
- [21] A. V. Savin, Y. S. Kivshar, and B. Hu. Suppression of thermal conductivity in graphene nanoribbons with rough edges. *Phys. Rev. B* **82**, 195422 (2010).
- [22] A. V. Savin and Y. S. Kivshar. Phononic Fano resonances in graphene nanoribbons with local defects. *Scientific Reports* **7**, Article number: 4668, (2017).
- [23] J.H. Los, J.M.H. Kroes, K. Albe, R.M. Gordillo, M.I. Katsnelson, and A. Fasolino. Extended Tersoff potential for boron nitride: Energetics and elastic properties of pristine and defective h-BN. *Phys. Rev. B* **96**, 184108 (2017).